Towards nano-injection molding using metallic glass tools

Nan Zhang, Cormac J. Byrne, David J. Browne, Michael D. Gilchrist*

School of Mechanical & Materials Engineering, University College Dublin, Belfield, Dublin 14, Ireland.
* michael.gilchrist@ucd.ie (Corresponding Author)

Bulk metallic glasses (BMGs), having no limiting microstructure, can be machined or thermoplastically-formed with sub-micron precision while still retaining often-desirable metallic properties such as high compressive strength. These novel materials thus have enormous potential for use as multi-scale tools for high-volume manufacturing of polymeric MEMS and information storage devices. Here we show the manufacture of a prototype BMG injection molding tool capable of producing cm-long polymeric components, with sub-micron surface features.

BACKGROUND

Micro-injection molding is widely used to form plastic components rapidly and precisely. Current tools for injection molding rely largely on tool steels for their strength and durability. The finite grain size in traditional crystalline metals means it is challenging to produce tools with features <10μm (Fig. 1b). However, the need for increasingly smaller featured plastic components is recognised, particularly for information storage and bio-analytical applications. For example, high volume production of millimetre to centimetre size components having features of dimensions ranging from the smallest virus (20nm) to mammalian cells (10μm), or the mid-section of the 'biological ruler' (Fig. 1a), could create new opportunities in the bio-analytical area.

Current developments in microsystems technology and trends in emerging products show there is an increasing requirement to integrate multi-scale functionality on progressively smaller platforms *(1)*. Typically, microfluidic devices for DNA/protein separation *(2-5)* and single DNA molecular manipulation *(6,7)* exhibit a series of micro-scale channels with integrated sub-micron and nanometre scale features. Producing such components and systems requires integrating manufacturing processes across the length scales from 10^{-2} to 10^{-7}m. Most of these devices are fabricated using silicon or glass so as to take advantage of well developed patterning technologies. To develop future applications and markets for microfluidic technologies, such as clinical, veterinary and point-of-care diagnostics, and both public health and environmental monitoring, will require large volumes of inexpensive products *(8)*. This will only be achieved using mass production methods. For a variety of reasons, including cost and material properties (e.g., optical, biocompatibility, good electrical insulation and excellent replication fidelity), polymers are gradually replacing silicon and glass for the fabrication of microfluidic devices *(9, 10)*. As micro-injection molding is a most cost-effective method for mass producing polymer micro-components, it is playing an increasingly important role in manufacturing microsystems.

Injection molding, as distinct from micro-injection molding, is used to form thermoplastic polymers on length scales ranging from 10^{0} to 10^{-5}m for applications

that range from the toy industry to micro gears in the watch industry. It has even been extended to the sub-micron ($\leq 10^{-6}$m) and nanometre scales ($\leq 10^{-7}$m). In order to maintain their functionality, all the micro/nano features of a fabricated polymer part must have high accuracy and good reproducibility, even whilst being manufactured in high volumes. However, interfacial effects, such as capillary forces, friction and entrapped air strongly influence the filling behaviour of micro/nano scale features. Premature solidification can occur because of the significant thermal diffusion rate associated with the high surface-to-volume ratio and reduced dimensions of micro/nano features; this usually prevents polymer melts from completely filling into micro/nano cavities. The friction and sticking force during the demolding process can also damage features which have relatively low mechanical properties *(11, 12)*. Process improvement and optimization, using ancilliary methods such as high-frequency induction mold heating systems *(13)*, cavity vacuum pumping systems *(14)* and functional coatings *(15)* can significantly improve the replication accuracy of micro/nano patterns in the injection molding process. These can extend the capability for precise replication with the injection molding process down to the sub-micron and nanometer scales.

Injection molding with sub-micron features is not unique. Polycarbonate CDs, DVDs and ultra high density blue-ray discs all have features with dimensions that extend from 500nm to 138 nm: these are typically manufactured using this process. Such operations often rely on the production of metal stamps which are ultimately derived from laser-etched glass master tools produced in a clean-room environment. Molding of polymer nanostructures down to 25nm in width and an aspect ratio of 2 has also been reported *(12, 16)*. These injection molding masters were either fabricated with silicon by lithographic methods, or as a replica relief by electroplating nickel onto a silicon wafer based master structure. However, tools fabricated directly from silicon are too brittle for high force and high volume applications *(17)*. The electroforming process of nickel microstructures as a metallic tool is slow and time consuming, and can not provide high aspect ratio features *(18)*. Nano-crystalline and sub micro-crystalline nickel shims have shown potential as tooling for sub micron and even nano-scale patterns *(19)*. However, their strength decreases from 1100MPa at room temperature to 100MPa at 350^{o}C *(20)* and therefore restricts applications for some plastics with high processing temperatures. There are also risks of the shim being damaged when high processing pressure is used in the injection molding process to improve filling of micro/nano features. An easily manufactured metallic alternative is clearly desirable.

Classes of metallic alloys, which resist crystallisation even at low cooling rates, were discovered in the mid-to-late 1980s (*21, 22*). These are bulk amorphous metals or bulk metallic glasses (BMGs), implying that all dimensions of the cast sample are >>1mm. Many alloy families and processing methods have been developed since their discovery (*23*). BMGs have combined properties, including high compressive strength, large elastic limit and excellent corrosion resistance, which markedly differentiate them from crystalline metals (*24, 25*). The often cited problem of brittleness has been overcome in some instances by carefully tailoring alloy composition (*26*). More recently, an extremely tough monolithic BMG with high yield strength has been discovered (*27*).

BMGs, being amorphous, have a microstructure of only several atomic lengths and thus can be patterned/machined to dimensions not easily obtained on conventional metals. A range of techniques for patterning BMGs has been demonstrated including direct casting, thermoplastic forming, and direct machining.

For conventional metals, using direct casting to form parts with small surface features is difficult, partially because of volume shrinkage associated with crystallisation, which is of the order of 5%. The low volume shrinkage associated with BMGs means they are better able to replicate mold features. Advances in the field of net-shape casting of BMGs have yielded dividends in terms of the range of geometries and part sizes that can be produced (*28*). However this method of surface patterning, whilst direct, is challenging when trying to replicate features in the single and sub-micrometer scales. Single roller techniques, used for decades to rapidly solidify thin metallic glass sections, can be used for surface patterning via direct or indirect patterning of the melt-spinning wheel. However the limited thickness of these sections (<100 μm) and the difficulty in controlling surface quality during rapid solidification, make this an impractical route for tooling applications. Twin-roll casting has recently been used to continuously produce large area BMG sheet, and this may point a way towards economical feedstock for multi-scale tooling applications (*29-31*).

When heated to above their glass transition temperature and below their crystallization temperature, into the range known as the supercooled liquid region, the viscosities of metallic glasses drop considerably and they can be molded in much the same way as thermoplastics. This unique characteristic allows BMGs to be formed into small and intricate shapes using many of the techniques applied to thermoplastic forming. Techniques such as die forging have been used successfully to produce freestanding micro-components (*29, 32*). However the geometries of such components are limited and high-fidelity replication of die surfaces poses practical engineering difficulties (*33*).

A significant amount of literature exists regarding direct embossing using patterned stamps. It has long been known that forming micrometer surface features on BMGs is possible (*18, 34-36*). Much of this work involves the use of expensive silicon master molds to form a child mold from BMG. Furthermore, the silicon master is sacrificial and must be etched away (e.g., in a heated KOH bath) for high aspect ratio feature replication. Such child molds, having mechanical properties superior to that of the silicon master, can then be used for micro-forming a large number of parts from other BMGs (with lower glass transition temperatures) or polymers. More recently, porous alumina has been used as a master to nano-pattern BMGs, with release taking place by dissolving the alumina (*20*). That work provided an interesting insight into the increasing dominance of surface tension of the supercooled liquid when carrying out thermoplastic forming with smaller scale features. The authors demonstrated that the correct choice of BMG and mold material allows feature formation down to 13 nm.

More recently, innovative forms of thermoplastic forming such as blow molding (*37*), and injection molding (*38*) have been described. In both of these cases, surface patterning of the BMG undergoing the forming can be achieved by placing a reverse pattern on the mold.

Kumar et al. *(39)* provided an extensive review of the state of the art in the use of BMGs for miniature applications. They conclude that applications on length scales from 1nm-5mm benefit most from the use of BMGs. At the lower end of this range, BMG devices, which target specific biomedical and information storage applications, will come to the fore (*40, 41*).

Direct machining can provide a controlled method of surface patterning BMGs. Conventional machining of certain BMGs is difficult and due to the brittleness of many alloys (*42*) great care must be exercised to avoid workpiece damage. Micro-scale and nano-scale machining of BMGs using techniques such as laser machining or focused ion beam (FIB) technology have been successfully demonstrated (*43-45*). Combined FIB and chemical etching has also been used to pattern BMGs (*46*).

CURRENT DEVELOPMENTS

The preceding discussion outlines why BMGs are viable materials to make robust, metallic, multi-scale tools (centimetre through nanometre) capable of producing high-volume, low-cost, nanometre-featured components. Other authors have previously suggested using BMGs as tools for micro-injection molding *(18, 20, 47)*. Some investigators have used these metallic glass tools to carry out micro-injection molding of microfluidic devices with 10^{-5} meter scale features *(48)*. It is worthwhile mentioning that the number of BMG alloys developed allow tailored properties for multi-scale tooling. Our aim here is to report results where we have reduced this to practice for a functional tool with features of the order of 10^{-7} meters. We have found little difficulty in replicating these features and believe that features of the order of 10^{-8} meters should be easy to replicate in high volumes.

A BMG multi-scale (10^{-2}m-10^{-7}m) injection-molding tool was fabricated in this work and used to injection mold plastic components. The tool was fabricated from a ternary BMG, with composition $Zr_{47}Cu_{45}Al_8$, via a drop-casting technique in an inert environment. X-ray diffraction (Fig. 2) confirmed the amorphicity of cylindrical ingots (5mm diameter, 40mm long). One BMG rod was machined into a flat dog-bone shape, polished and mounted as an insert into a steel die. The average surface roughness after polishing is 160nm with standard deviation of 17nm. The die was designed to slot into the fixed face of a mold cavity in a Fanuc Roboshot 2000i15B micro-injection molding machine. The moving side of the mold (producing the ribbed face of the part shown in Fig. 1c) was made from steel. The BMG thus acted as the forming face for the non-ribbed side of the polymeric part (underside of the part in Fig. 1c).

The BMG insert was both micro- and sub micron-patterned. Features on the scale of 10^{-5}m to 10^{-7}m were machined into the BMG using FIB milling with an FEI Quanta 3D FEG DualBeam FIB (30keV Ga^+ ion beam and a current of 1nA, from bottom to top and 1μs dwell time). Features machined using this technique are shown in Fig. 1c. A series of ridges and grooves were machined parallel and perpendicular to the melt flow direction in the injection molding cavity. The smallest of the grooves was 250nm wide. A complex UCD crest-pattern was also machined, with ~150nm spaced harp strings.

The BMG tool could have been fabricated using several other routes as outlined previously, such as direct casting or thermoplastic forming. However, a centimetre

scale tool was required with features down to 10^{-7}m. Near net-shape casting followed by conventional machining and then FIB machining of the micrometer and sub-micrometer features was the most direct route for tool manufacture. This route was also an economical route for fabricating this tool. The practical difficulty of FIB machining of common tool steel is shown in Fig. 1b. The benefit of using a BMG is obvious also in this figure, where a sharply defined cog pattern can be readily machined into the BMG.

Using non-optimised molding conditions it was easy to produce HDPE (HMA 016) parts as shown in Fig. 2c, with good replication of all features including the 150nm harp strings. The process conditions were as follows: injection speed 500mm/s, holding pressure 50MPa, holding time 0.5s, melt temperature 160^{o}C, mold temperature 60^{o}C. The cycle time is less than 10s. The orientation of features relative to the melt flow, as well as their aspect ratio, particularly when molding positive plastic motifs, affected the sharpness of replication. This absence of process optimisation (temperatures, compression cycle, optimum polymer, etc.) indicates that higher fidelity replication of the smallest features is potentially possible. Simple modelling dictates that even smaller features with larger aspect ratios can be transferred to plastics, given the correct processing conditions. Our experiments also indicate that all the sub-micron patterns can be maintained over 20000 molding cycles.

We also explored the nanometer scale replication capabilities of BMG. We designed an array of square pillars to gradually extend the cavity dimensions to the nanometer scale (~200nm). A designed bitmap was used when FIB milling to machine square cavities on the surface of BMG. By varying the dimensions of the bitmap, the length of the sides of the individual square cavities was varied from ~400nm to ~200nm. By using different FIB milling strategies, the three arrays of 8×8 square cavities (Fig 3a) each had different depths on an area of 6μm×6μm. A BMG pillar array was also machined with FIB on the inside of a 3μm×3μm cavity (Fig. 3b). 8×8 square cavity arrays in an area of 3μm×3μm were also easily patterned on the surface of BMG (Fig. 3c); the length of the sides of these squares was ~200nm. It was not possible in our experimental trial to use FIB milling to pattern the square cavity arrays down to ~100nm. However, a nano-porous array with pore diameter of ~100nm was machined based on pixels on the bitmap, in which each pixel was regarded as a fabrication dot (c.f. 4×4 array of pores shown in Fig. 3d). Micro-injection molding with this BMG tool successfully exhibited its capability for multi-scale replication and all the defined patterns on BMG were well replicated without process optimization even with the smallest ~100nm features, as seen in Fig. 3e-h. The replication fidelity could be enhanced with process optimization and by using auxiliary equipment.

Although its amorphous structure means that metallic glasses can be used for multi-scale patterning, it also means that BMGs can be strong but brittle. Ultra-fine polishing of BMGs is possible although the science behind such polishing is not well developed. Some micro products, such as micro contact lens for flat panel displays *(49)*, nanophotonic components, information storage media, such as blue ray disks, and some bio-analytical applications, require mirror grade surface finishes. In addition, the replication of micro/nano features is also sensitive to surface roughness, due to its effect on heat transfer and local flow fields *(50)*. We attempted to use conventional lapping and polishing methods to provide a mirror grade finish on a BMG tool. As shown in Fig. 4a, four strips of BMG were polished to an average surface roughness

of ~9nm and then assembled into both sides of a square plate cavity. Under process conditions of injection mold temperature 50^{o}C, injection velocity 50 mm/s, nozzle temperature 205 ^{o}C and holding pressure 35MPa, the micro molded part in PMMA (Altuglas VSUVT-100) exhibited an average roughness of ~6nm. Some flaws such as tiny white dimples are visible on the clear surface: these are due to pores on the surface of the BMG strips from the metal casting process. We are currently working on methods to avoid and/or remove such microporosity.

FUTURE PROSPECTS

This new metallic-glass based sub-micron injection molding technique offers an exploitable opportunity for high-volume, low-cost, micro- and nano-fabrication of polymers. Given the span in length scale that can be produced on a single part (10^{-2} m-10^{-7}m), it is anticipated that this technology will find applications in the field of medical diagnostics. Additionally, if the length scales can be reduced to 10^{-8}m, a platform for high-volume, low-cost, information storage systems are within reach. Optimization of the processing conditions will assist in this endeavour.

Future challenges from a materials perspective will centre on rational choices of alloys for specific applications such that properties (including strength, fatigue resistance, toughness, thermal conductivity and machinability) can be tailored to specific tooling. Although we have described BMG tools that we have used for in excess of 20,000 injection molding cycles, the lifetime of these tools under such conditions is not obvious and warrants further study. The correct choice of alloy will undoubtedly allow the useful tool-life to be optimized. Such optimization will be helped by the current rapid expansion in knowledge surrounding amorphous metals.

ACKNOWLEDGEMENTS

The authors gratefully acknowledge financial support from the Chinese Scholarship Council and Enterprise Ireland (Grants CFTD/07/314 & CFTD/06/IT/335), as well as technical assistance from Dr Ian Reid (NIMAC-UCD) with microscopy and FIB machining.

References

(1) E.B. Brousseau et al, (2010), *Int. J. Adv. Manuf. Tech.*, **47**, 161-180
(2) J. Han et al, (2000), *Science*, **288**, 1026-1029
(3) M. Baba et al, (2003), *Appl. Phys. Lett.*, **83**, 1468-1470
(4) L.R. Huang et al, (2004), *Science*, **304,** 987-990
(5) J. Fu et al, (2007), *Nat. Nanotechnol.*, **2**,121-128
(6) H. Craighead, (2006), *Nature*, **422**, 387-393
(7) J.T. Mannion et al, (2006), *Biophys. J* ,4538-4545
(8) G.M. Whitesides,(2006). *Nature*, **442**, 368-373
(9) U.M. Attia et al, (2009), *Microfluid Nanofluid*, **7**, 1-28
(10) Yole Développement, *Microfluidic substrates market and processing trends*. (2011)
(11) S. Scholz, *PhD thesis*, Cardiff University, (2011)
(12) M. Matschuk, et al, (2010), *Microelectron. Eng*, **87**, 1379–1382
(13) K. Park et al, (2010), *J Micromech Microeng*., **20**, 035002
(14) H. Yokoi, et al, (2006), *Polym. Eng. Sci.*, **46**, 1140–1146
(15) H. Pranov, et al, (2006), *Polym. Eng. Sci.*, **46**,160-171
(16) H. Schift, et al, (2000), *Microelectron. Eng*, **53**, 171-174

(17) J. Greener, R. Wimberger-Friedl, *Precision injection molding: Process, materials and applications*. Hanser Gardner Publications, Munich, (2006)
(18) D.L. Henann et al, (2009), *J. Micromech. Microeng*, **19**, 115030
(19) H. Hosokawa et al, (2004), *Philos. Mag. Lett.*, **84**,713-718
(20) G. Kumar et al, (2009), *Nature*, **457** , 868-872
(21) A. Inoue et al, (1989), *Mater. Trans. JIM*, **30**, 965-972
(22) H.W. Kui et al, (1984), *Appl. Phys. Lett.*, **45**, 615-616
(23) C.J. Byrne, M. Eldrup, (2008), *Science*, **321**, 502-503
(24) A.R. Yavari et al, (2007), *MRS Bulletin*, **32**, 635-638
(25) A.L. Greer, (2009), *Mater. Today*, **12**, 14-22
(26) Liu et al, *Science* (2007), **315**, 1385-1388
(27) M.D. Demetriou et al, (2011), *Nature Mater.*, **10**, 123–128
(28) J.J. Wall et al, (2006), *Rev. Sci. Instr.*, **77**, 033902
(29) Z. Zhang and J. Xie, (2006), *Mat. Sci. Eng. A*, **433**, 323–328
(30) G. Duggan et al, (2009), *Trans. Indian Inst. Met.*, **62**, 417-421
(31) D. East et al, (2010), *Materials Science Forum*, **654-656**, 1078
(32) J.A. Wert et al, (2009), *J. Mater. Process. Technol.*, **209**, 1570–1579
(33) C.J. Byrne et al, (2010), *J. Mater. Process. Technol.*, (2010), **210**, 1419–1428
(34) Y. Saotome et al, (2002), *Intermetallics*, **10**, 1241–1247
(35) N.H. Pryds, (2004), *Mater. Sci. Eng. A*, **186**, 375–377
(36) J.P Chu et al, (2007), *Appl. Phys. Lett.*, **90**, 034101
(37) J. Schroers et al, (2007), *Scripta Mater.*, **57**, 341
(38) A. Wiest et al, (2009), *Scripta Mater.*, **60**, 160-163
(39) Kumar et al, (2011), *Adv. Mater.*, **23**, 461–476
(40) M.F. Ashby, A.L. Greer, (2006), *Scripta Mat.*, **54**, 3, 321-326
(41) J. Schroers et al, (2009), *JOM*, **61**, 9, 21-29
(42) S. H. Yeo et al, (2009) *Mat. Man. Proc.*, **24**, 12
(43) S.N. Aqida et al, (2010), *App. Phys. A*, **101**, 2, 357-360
(44) Y. Saotome et al, (2007), *Mater. Sci. Forum*, **2088**, 539–543
(45) D.J. Stratton et al, (2011), *MRS Proceedings*, **1300**, mrsf10-1300-u02-08
(46) N. Kawasegi et al, (2007), *Nanotechnology*, **18**, 375302
(47) A. A. Kündig et al, (2003), *Microelec. Eng.*, **67-68**, 405-409
(48) G. Fu et al, (2011), *Microsyst Technol.*, **17**, 1791–1798
(49) C. Weng et al, (2010), *J. Micromech. Microeng.*, **20**, 035033
(50) H.L. Zhang et al, (2007), *Polym. Eng. Sci.*, **47**, 2012–2019

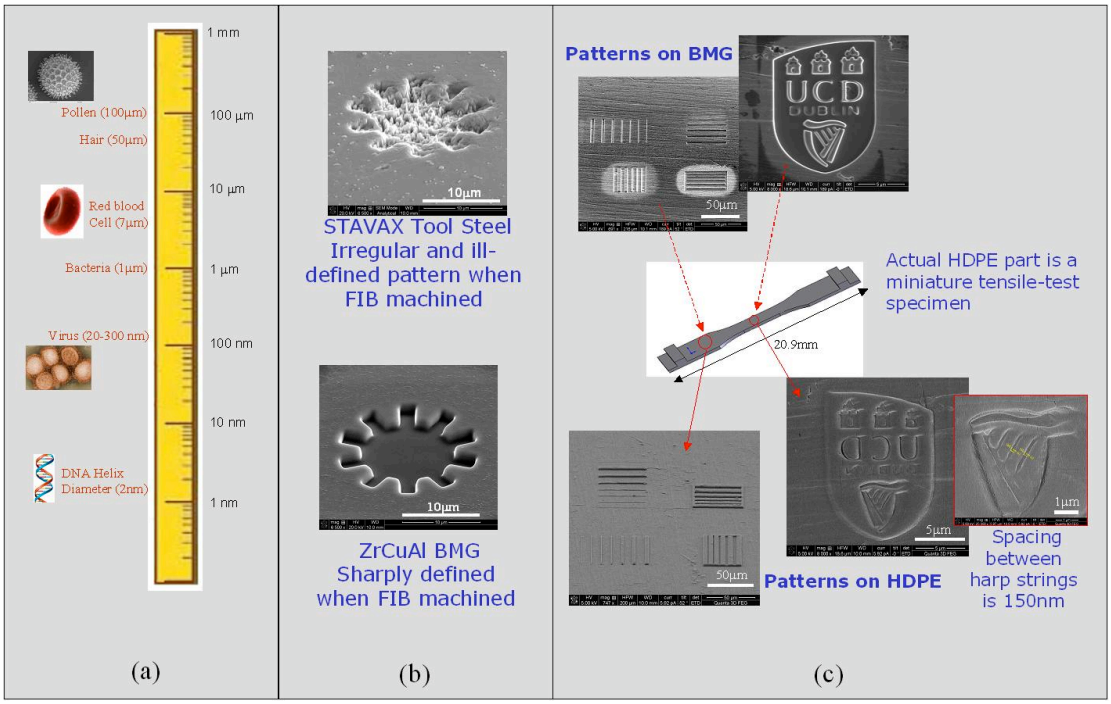

Fig. 1:

(a) Illustrative biological length scales. Using this technology, features from cm scale (dog-bone in pane (c)) down to virus' diameters can be replicated on polymers at high-speed.

(b) Ion-beam machining of common fine-grained crystalline tool steel with features below length scale of grains results in an ill-defined pattern on tool. Using amorphous metal, which has no limiting micro-structural length scale, a sharply defined pattern can be produced.

(c) A series of grooves and channels and UCD crest machined into BMG dog-bone shaped tool. The maximum channel width is 2µm and smallest width is 250nm. The spacing between the harp strings on the crest is 150nm. The tool is used to injection mold 20.9mm long dog-bone shaped parts. The FIB machined features, including the 150nm wide harp strings illustrated, are well replicated without much optimisation of the molding process.

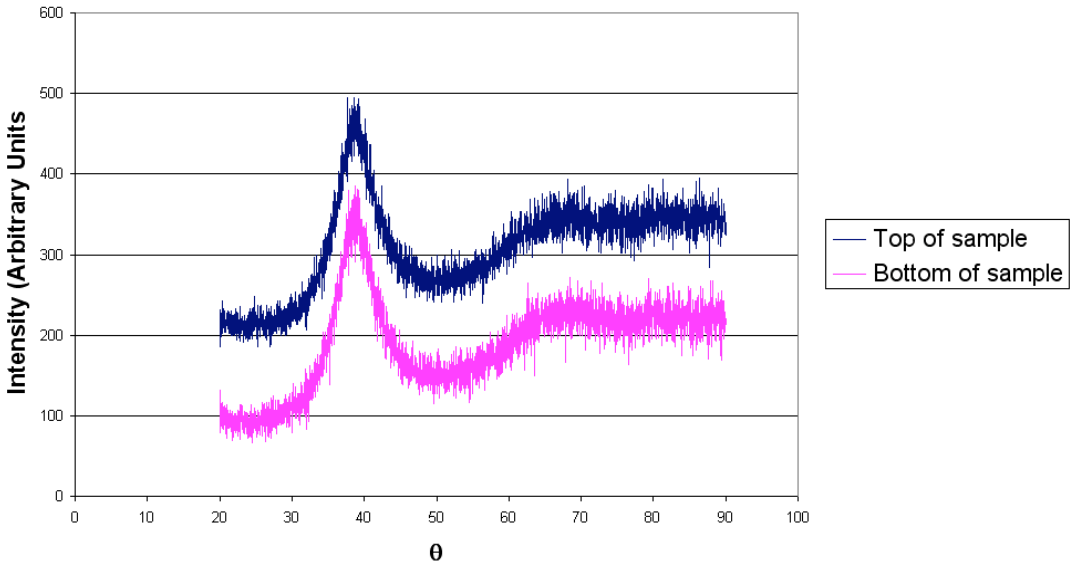

Fig. 2:

XRD scan of the top and bottom of the 5-mm diameter, 40-mm long cast rod, indicating the amorphicity of the sample.

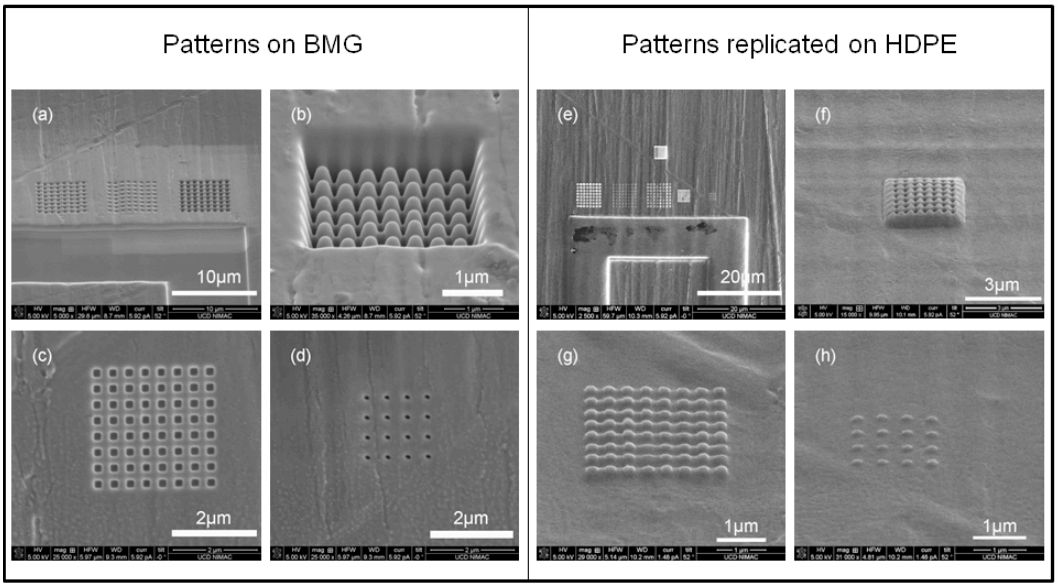

Fig. 3:

(a) ~400nm square cavity arrays with different depths, which are machined with different FIB milling process settings: 30kV beam voltage, 0.3nA beam current, with out-of-plane dimension (i.e., depth) of 100nm, 50nm and 200nm from left to right. The area of each 8×8 array is 6μm×6μm. All these features are located near a ~10μm wide micro channels, which was machined with a 30kV beam voltage and 5.0nA beam current.

(b) Sub-micron array of BMG pillars (7×7) inside a 3μm×3μm micro cavity machined with 30kV beam voltage and 1nA beam current.

(c) Plan view of 8×8 square cavity array with area of 3μm×3μm with length and width of the sides of each square ~200nm. The squares were sharply patterned with FIB milling on BMG.

(d)~100nm array of holes made by FIB milling with a 30kV beam voltage and a 30pA beam current.

(e) Overview of replicated sub-micron scale features (c.f. Fig. 3a) using the injection molding process.

(f) Replicated 3 μm×3μm pillar with sub-micron holes on its top (c.f. Fig. 3b).

(g) Replicated 8×8 square pillar array (c.f. Fig. 3c); width of each pillar ~200nm.

(h) Replicated sub-micron cone array (c.f. Fig. 3d).

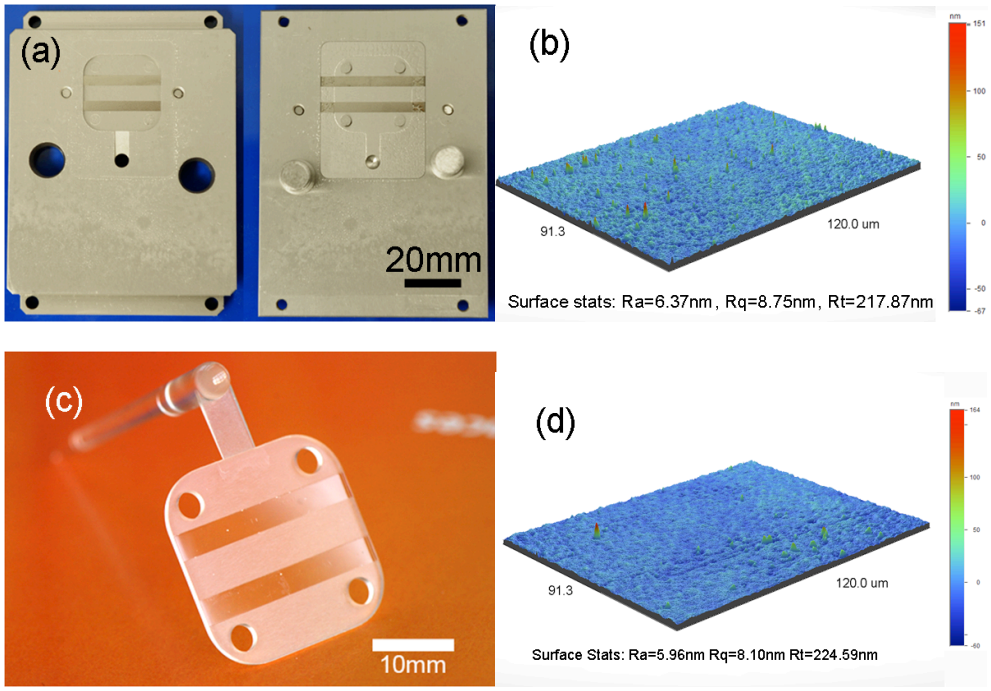

Fig. 4:

(a) square plate mold with both halves incorporating two BMG strips.

(b) 3-dimensional representation of surface finish on typical area of BMG. The roughness in this area ranges from Ra = 5 to 8nm.

(c) molded PMMA square part with optically clear strip surface replicated from the BMG inserts.

(d) 3-dimensional representation of surface finish of optical surface of PMMA part. The surface roughness in this area ranges from Ra = 5 to 11nm.